J|A|C|S
ARTICLES
Published on Web 02/20/2002

Fluorescence Enhancement of *trans*-4-Aminostilbene by *N*-Phenyl Substitutions: The "Amino Conjugation Effect"

Jye-Shane Yang,* Shih-Yi Chiou, and Kang-Ling Liau

Contribution from the Department of Chemistry, National Central University, Chung-Li, Taiwan 32054

Received June 14, 2001. Revised Manuscript Received October 31, 2001

Abstract: The synthesis, structure, and photochemical behavior of the trans isomers of 4-(*N*-phenylamino)-stilbene (**1c**), 4-(*N*-methyl-*N*-phenylamino)stilbene (**1d**), 4-(*N,N*-diphenylamino)stilbene (**1e**), and 4-(*N*-(2,6-dimethylphenyl)amino)stilbene (**1f**) are reported and compared to that of 4-aminostilbene (**1a**) and 4-*N,N*-dimethylaminostilbene (**1b**). Results for the corresponding 3-styrylpyridine (**2**) and 2-styrylnaphthalene analogues (**3**) are also included. The introduction of *N*-phenyl substituents to 4-aminostilbenes leads to a more planar ground-state geometry about the nitrogen atom, a red shift of the absorption and fluorescence spectra, and a less distorted structure with a larger charge-transfer character for the fluorescent excited state. Consequently, the *N*-phenyl derivatives **1c**−**e** have low photoisomerization quantum yields and high fluorescence quantum yields at room temperature, in contrast to the behavior of **1a**, **1b**, and most unconstrained monosubstituted *trans*-stilbenes. The isomerization of **1c** and **1d** is a singlet-state process, whereas it is a triplet-state process for **1e**, presumably due to a relatively higher singlet-state torsional barrier. The excited-state behavior of **1f** resembles **1a** and **1b** instead of **1c**−**e** as a consequence of the less planar amine geometry and weaker orbital interactions between the *N*-phenyl and the aminostilbene groups. Such an *N*-phenyl substituent effect is also found for **2** and **3** and thus appears to be general for stilbenoid systems. The nature of this effect can be described as an "amino conjugation effect".

Introduction

Studies on substituent effects continue to provide insights into the excited states of stilbenes and related systems.[1−7] Two decay processes, fluorescence and trans → cis isomerization, account for the excited-state behavior of *trans*-stilbene and most substituted stilbenes in solution. Isomerization can occur via either the singlet or the triplet state, depending on the nature of substituents. The triplet-state mechanism is important for some halogen-, nitro-, and carbonyl-substituted stilbenes, but the singlet-state mechanism is dominant for *trans*-stilbene and other substituted stilbenes. Double bond torsion for singlet-state isomerization involves a thermal barrier between the planar (^{1}t*) and the perpendicular (^{1}p*) states. The barrier height and the temperature thus determine the quantum yields of fluorescence vs isomerization when intersystem crossing is negligible in the excited-state decay. For example, in the case of *trans*-stilbene a torsional barrier of ∼3.5 kcal/mol corresponds to a fluorescence yield of 3−5% and a nearly maximum of trans → cis yield of ∼50% at room temperature.[3] Substituents can, in principle, raise the torsional barrier and thus the fluorescence quantum yield by lowering the energy of the fluorescent ^{1}t* state more than that of the ^{1}p* state. However, the undefined nature of the ^{1}p* state precludes effective prediction of the substituent effect on the torsional barrier and the fluorescence efficiency of *trans*-stilbenes. A literature survey reveals that, except for π-substituents such as phenyl[8] or styryl[9] groups that extend the conjugation length, neither electron-withdrawing nor electron-donating substituents can lead to fluorescence as the dominant mode of excited-state decay (>50%) for unconstrained and 4-substituted *trans*-stilbenes at room temperature.[1−3]

It has recently been recognized that *N*-phenyl vs *N*-alkyl substitution of aromatic amines can lead to superior performance in materials chemistry.[10−14] Examples include improvement in thermal stability,[10] molecular hyperpolarizability,[10−12] and hole

* To whom correspondence should be addressed. E-mail: jsyang@cc.ncu.edu.tw.

(1) Görner, H.; Kuhn, H. J. *Adv. Photochem.* **1995**, *19*, 1−117.
(2) Waldeck, D. H. *Chem. Rev.* **1991**, *91*, 415−436.
(3) (a) Saltiel, J.; Waller, A. S.; Sears, D. F., Jr.; Hoburg, E. A.; Zeglinski, D. M.; Waldeck, D. H. *J. Phys. Chem.* **1994**, *98*, 10689−10698. (b) Saltiel, J.; Waller, A. S.; Sears, D. F., Jr.; Garrett, C. Z. *J. Phys. Chem.* **1993**, *97*, 2516−2522. (c) Saltiel, J., Sun, Y.-P. *Photochromism, Molecules and Systems*; Dürr, H., Bouas-Laurent, H., Eds.; Elsevier: Amsterdam, 1990; pp 64−164. (d) Saltiel, J.; Charlton, J. L. *Rearrangements in Ground and Excited States*, de Mayo, P., Ed.; Academic Press: New York, 1980; Vol. 3, pp 25−89.
(4) Lewis, F. D.; Yang, J.-S. *J. Am. Chem. Soc.* **1997**, *119*, 3834−3835.
(5) Lewis, F. D.; Kalgutkar, R. S.; Yang, J.-S. *J. Am. Chem. Soc.* **1999**, *121*, 12045−12053.
(6) Lewis, F. D.; Weigel, W. *J. Phys. Chem. A* **2000**, *104*, 8146−8153.
(7) Lewis, F. D.; Weigel, W.; Zuo, X. *J. Phys. Chem. A* **2001**, *105*, 4691−4696.
(8) Bokeriya, É. N.; Viktorova, V. S.; Karegishvili, L. I.; Kovyrzina, K. A.; Kushakevich, Y. P.; Radaikina, L. A. *J. Org. Chem. USSR (Engl. Transl.)*, **1979**, *15*, 1944−1949.
(9) Nakatsuji, S.; Matsuda, K.; Uesugi, Y.; Nakashima, K. Akiyama, S.; Katzer, G.; Fabian, W. *J. Chem. Soc., Perkin Trans. 2* **1991**, 861−867.
(10) (a) Bedworth, P. V.; Cai, Y.; Jen, A.; Marder, S. R. *J. Org. Chem.* **1996**, *61*, 2242−2246. (b) Verbiest, T.; Burland, D. M.; Jurich, M. C.; Lee, V. Y.; Miller, R. D.; Volksen, W. *Science* **1995**, *268*, 1604−1606. (c) Gilmour, S.; Montgomery, R. A.; Marder, S. R.; Cheng, L.-T.; Jen, A. K.-Y.; Cai, Y.; Perry, J. W.; Dalton, L. R. *Chem. Mater.* **1994**, *6*, 1603−1604. (d) Marder, S. R.; Perry, J. W. *Science* **1994**, *263*, 1706−1707.
(11) Whitaker, C. M.; Patterson, E. V.; Kott, K. L.; McMahon, R. J. *J. Am. Chem. Soc.* **1996**, *118*, 9966−9973.

10.1021/ja016416+ CCC: $22.00

mobility[13,14] of arylamines when applied for nonlinear optics or in organic electroluminescent devices. On the basis of theoretical studies, the influence of *N*-phenyl substitutions has been attributed to a more planar amine structure and to a nonconventional "conjugation" between the aryl and the introduced phenyl groups.[11,13] In comparison to these ground-state properties, the *N*-phenyl substituent effect on the excited-state behavior of arylamines is less investigated.[15] In particular, while the excited states of aminostilbenes and their *N*,*N*-dimethyl derivatives have been extensively investigated,[4−7,16−18] little attention has been paid to their *N*-phenyl-substituted counterparts. Moreover, several *N*,*N*-diaryl derivatives of *trans*-4-aminostilbenes have been investigated as solid-state electroluminescent materials and shown to have high luminescent efficiency;[19] however, no fluorescence quantum yield data were reported. This behavior is in complete contrast to the inherently weak fluorescence of both *trans*-4-aminostilbene (**1a**)[5] and *trans*-4-*N*,*N*-dimethylaminostilbene (**1b**).[16] In this context, we have investigated the *N*-phenyl substituent effect on the excited-state behavior of aminostilbenes. We report herein that the fluorescence of **1a** and **1b** in solutions is dramatically increased by more than 1 order of magnitude upon *N*-phenyl (**1c**,**d**) or *N*,*N*-diphenyl (**1e**) substitutions. We attribute this to an "amino conjugation effect" on the basis of the absence of fluorescence enhancement in the case of **1f**, where the "conjugation" between the stilbene and the phenyl group is interrupted or diminished. Similar effects are also observed for the *trans*-1,2-diarylethylenes **2** and **3** and thus appears to be general for stilbenoid systems. The origin of this "amino conjugation effect" on fluorescence as well as other excited-state properties will be elucidated and discussed.

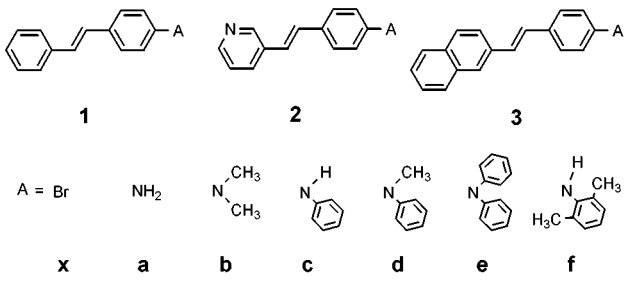

Scheme 1

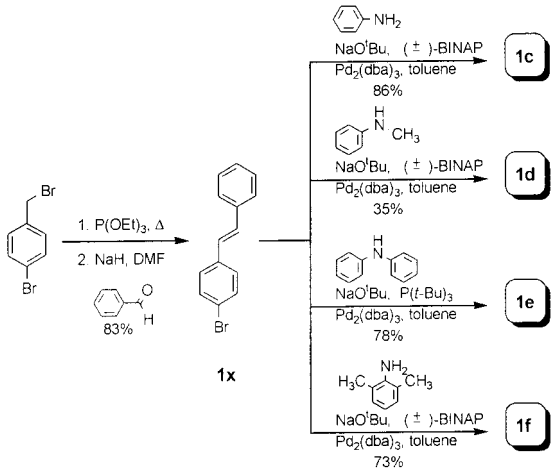

Results and Discussion

Molecular Structure. The recent development of palladium-catalyzed aromatic carbon−nitrogen bond formation[20] provides a feasible method for the synthesis of *N*-phenylamino- and *N*,*N*-diphenylamino-substituted stilbenes and 1,2-diarylethylenes.[21] As is shown in Scheme 1, the $Pd_2(dba)_3$/(±)-BINAP/NaOBu^t catalyst system[22] was employed for the coupling of *trans*-4-bromostilbene (**1x**) and corresponding amines in toluene solution to afford **1c**, **1d**, and **1f**. Compound **1e** was prepared under slightly different conditions, in which the ligand (±)-BINAP was replaced by P(*t*-Bu)$_3$.[23] The same method was also applied to the formation of compound series **2** and **3** by replacing **1x** with *trans*-3-(4-bromostyryl)pyridine (**2x**) and *trans*-2-(4-bromostyryl)naphthalene (**3x**), respectively. The precursors **1x**−**3x** were in turn prepared according to the standard Horner−Wadsworth−Emmons procedures for olefin synthesis.[24]

The ground-state structures of **1a**−**f** have been investigated by MOPAC−AM1 calculations.[25] Compounds **1c**, **1d**, and **1f** are structurally unsymmetrical and can adopt either one of two planar conformations as a consequence of rotation about the styrene-diphenylamine single bond. As is depicted for **1c** (eq 1), the conformer **1c-syn**, which has both the *N*-phenyl and

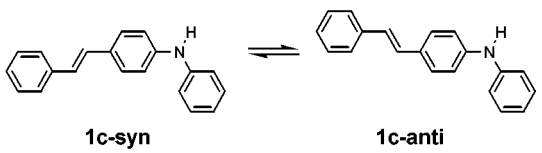

(1)

styrene groups located on the same side with respect to the long molecular axis, is slightly lower in energy by 0.29 kcal/mol than the other conformer **1c-anti**. The syn conformers of both **1d** and **1f** were also calculated to have a lower energy than the corresponding anti conformers with energy differences similar to that for **1c** (Table 1).

(12) Moylan, C. R.; Twieg, R. J.; Lee, V. Y.; Swanson, S. A.; Betterton, K. M.; Miller, R. D. *J. Am. Chem. Soc.* **1993**, *115*, 12599−12600.
(13) Sakanoue, K.; Motoda, M.; Sugimoto, M.; Sakaki, S. *J. Phys. Chem. A* **1999**, *103*, 5551−5556.
(14) (a) Pacansky, J.; Waltman, R. J.; Seki, H. *Bull. Chem. Soc. Jpn.* **1997**, *70*, 55−59. (b) Kitamura, T.; Yokoyama, M. *J. Appl. Phys.* **1991**, *69*, 821−826.
(15) Rumi, M.; Ehrlich, J. E.; Heikal, A. A.; Perry, J. W.; Barlow, S.; Hu, Z.; McCord-Maughon, D.; Parker, T. C.; Röckel, H.; Thayumanavan, S.; Marder, S. R.; Beljonne, D.; Brédas, J.-L. *J. Am. Chem. Soc.* **2000**, *122*, 9500−9510.
(16) Létard, J.-F.; Lapouyade, R.; Rettig, W. *J. Am. Chem. Soc.* **1993**, *115*, 2441−2447.
(17) Papper, V.; Pines, D.; Likhtenshtein, G.; Pines, E. *J. Photochem. Photobiol. A Chem.* **1997**, *111*, 87−96.
(18) (a) Lewis, F. D.; Kalgutkar, R. S. *J. Phys. Chem. A* **2001**, *105*, 285−291. (b) Il'ichev, Y. V.; Kühnle, W.; Zachariasse, K. A. *Chem. Phys.* **1996**, *211*, 441−453. (c) Lapouyade, R.; Kuhn, A.; Letard, J.-F.; Rettig, W. *Chem. Phys. Lett.* **1993**, *208*, 48−58. (d) Gruen, H.; Görner, H. *J. Phys. Chem.* **1989**, *93*, 7144−7152.
(19) (a) Adachi, C.; Tsutsui, T.; Saito, S. *Appl. Phys. Lett.* **1990**, *56*, 799−801. (b) Adachi, C.; Tsutsui, T.; Saito, S. *Appl. Phys. Lett.* **1990**, *56*, 531−533. (c) Adachi, C.; Tsutsui, T.; Saito, S. *Appl. Phys. Lett.* **1989**, *55*, 1489−1491.
(20) (a) Wolfe, J. P.; Wagaw, S.; Marcoux, J.-F.; Buchwald, S. L. *Acc. Chem. Res.* **1998**, *31*, 805−818. (b) Hartwig, J. F. *Angew. Chem., Int. Ed.* **1998**, *37*, 2046−2067.
(21) See Supporting Information for details.
(22) Wolfe, J. P.; Buchwald, S. L. *J. Org. Chem.* **2000**, *65*, 1144−1157.
(23) Yamamoto, T.; Nishiyama, M.; Koie, Y. *Tetrahedron Lett.* **1998**, *39*, 2367−2370.
(24) Wadsworth, W. S., Jr. *Org. React.* **1977**, *25*, 73−253.
(25) Dewar, M. J. S.; Zoebisch, E. G.; Healy, E. F.; Stewart, J. J. P. *J. Am. Chem. Soc.* **1985**, *107*, 3902−3909.

Table 1. AM1-Calculated Heats of Formation (ΔH_f), Sum of Bond Angles (θ) about the N Atom, and Dihedral Angles (α) between the *N*-Phenyl Planes for **1a**−**f**

	1a	1b	1c	1d	1e	1f
ΔH_f (kcal/mol)	59.01	69.54	95.35 (95.64)[a]	103.91 (104.19)[a]	137.30	83.80 (84.11)[a]
θ (degree)	342.9	351.6	353.9	357.3	360.0	347.8
α (degree)			50	53	56 (59)[b]	71

[a] Value in parentheses is for the anti conformer (eq 1). [b] Value in parentheses is for the second *N*-phenyl substituent vs *N*-phenyl of stilbene group.

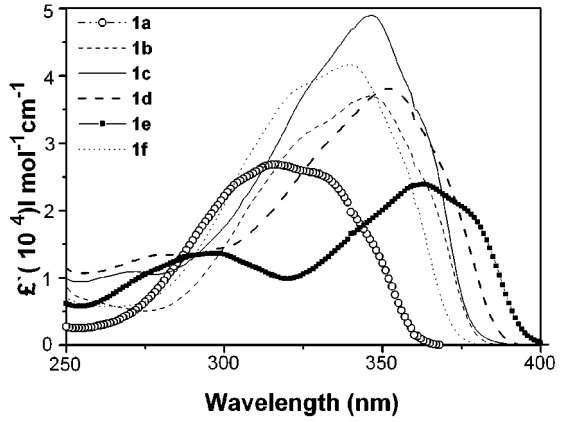

Figure 1. UV-vis absorption spectra of **1a**−**f** in hexane.

The structural differences in the amine groups among **1a**−**f** can be described by two parameters: the sum of bond angles (θ) about the N atom for all cases and the dihedral angle (α) between the two *N*-phenyl planes of the amine groups for **1c**−**f** (Table 1). We would expect a larger orbital overlap among the amine nitrogen, the *N*-phenyl, and the stilbene groups when the θ value is closer to 360° and the α value to 0°. AM1-calculations suggest that the θ value for aminostilbenes increases upon both *N*-alkyl and *N*-phenyl substitutions, but this effect is in the order *N*-phenylation > *N*-alkylation (i.e., **1e** > **1d** > **1c** > **1b**). Similar results have been observed for aniline derivatives,[13] but the θ values are aminostilbenes > anilines with the same amine substituents (e.g., **1a** (342.9°) > aniline (335.2°) and **1d** (357.3°) > methyldiphenylamine (351.8°)) (Table 1). However, both **1e** and triphenylamine[11] attain completely planar structures about the N atom ($\theta = 360°$)(i.e., a sp^2 character for the N atom). These results indicate that the more of the larger aryl groups the amine contains, the more planar structure about the N atom and thus the better the delocalization of the amine lone pair electrons to the π-systems. The calculated α value for **1c** is 50°. Slightly larger values of α are obtained for **1d** and **1e**, presumably due to the bulkier amine groups (Table 1). In comparison to **1c**, the introduction of methyl substituents at the ortho positions of the *N*-phenyl group (**1f**) not only increases the dihedral angle α but also decreases the θ value. Results from X-ray crystallography for related *N*-phenyl-substituted aminostilbenes that form single crystals indeed agree with the AM1-predicted syn conformations and θ and α values.[26]

Absorption Spectra. The absorption spectra of **1c**−**f** in hexane are shown in Figure 1. For comparison, the spectra of **1a**[5] and **1b**[16] in hexane are included. Except for **1e**, which possesses a second absorption band at shorter wavelengths, these molecules have a single intense long wavelength band, resembling those of *trans*-stilbene and other 4-substituted stilbenes.[27] The introduction of *N*-phenyl substituents in **1a** results in considerable bathochromic and hyperchromic shifts, suggesting substantial interactions between the *N*-phenyl and aminostilbene groups. Indeed, it has been suggested for triphenylamine and its derivatives that there is conjugation between the nitrogen lone pair electrons and the phenyl π-electrons, and that the whole molecule is a new chromophore with characteristic absorption and emission spectra.[28] The second band near 300 nm for **1e** is a consequence of an electronic transition mainly localized in the triphenylamine moiety,[29] which is supported by the results of semiempirical INDO/S−SCF−CI (ZINDO) calculations (vide infra).[30]

Table 2. Maxima of UV Absorption (λ_{abs}) and Fluorescence (λ_{fl}), Fluorescence-Band Half-Width ($\Delta\nu_{1/2}$), 0,0 Transition ($\lambda_{0,0}$), and Stokes Shifts ($\Delta\nu_{st}$) of Aminostilbenes **1**−**3** in Hexane and Acetonitrile

compd	solvent	λ_{abs} (nm)[a]	λ_{fl} (nm)[b]	$\Delta\nu_{1/2}$ (cm^{-1})	$\lambda_{0,0}$ (nm)	$\Delta\nu_{st}$ (cm^{-1})[c]
1a[d]	hexane	316	(361) 380	3580	354	5330
	acetonitrile	318	423	3418	378	7806
1b[e]	hexane	347	379 (400)	3425	370	2433
	acetonitrile	351	440	3306	394	5763
1c	hexane	346	378 (397)	2813	369	2447
	acetonitrile	351	436	3263	389	5554
1d	hexane	352	385 (404)	2619	378	2435
	acetonitrile	354	450	3753	395	6062
1e	hexane	362 (295)	395 (417)	2475	387	2307
	acetonitrile	362 (297)	455	3368	402	5646
1f	hexane	341	375 (395)	3381	365	2659
	acetonitrile	347	424	3370	384	5233
2a[f]	cyclohexane	336	390			4121
	acetonitrile	342	446			6818
2c	hexane	352	385 (405)	2729	376	2435
	acetonitrile	358	456	3217	402	6003
2e	hexane	358 (297)	403 (425)	2433	396	3119
	acetonitrile	367 (294)	476	3370	414	6239
2f	hexane	346	383 (402)	3169	373	2792
	acetonitrile	351	450	3149	396	6268
3a[f]	cyclohexane	342	392			3730
	acetonitrile	348	451			6562
3c	hexane	355	388 (407)	3274	380	2396
	acetonitrile	361	455	3353	406	5723
3e	hexane	371 (301)	405 (426)	2781	396	2263
	acetonitrile	371 (298)	489	3300	416	6504
3f	hexane	350	385 (403)	3360	378	2597
	acetonitrile	356	450	3526	398	5868

[a] The second absorption band in parentheses. [b] The second vibronic band in parentheses. [c] $\Delta\nu_{st} = \nu_{abs} - \nu_{fl}$. [d] From ref 5, except values for $\Delta\nu_{1/2}$ and $\Delta\nu_{st}$. [e] From ref 16. [f] From ref 4.

In comparison of compound series **1**−**3** in hexane and acetonitrile are reported in Table 2. It is interesting to note that the absorption maxima of **1b** and **1c** are essentially identical, and that the extent of the red shift of the absorption maxima for **1a**−**f** (i.e., **1a** < **1f** < **1b** ∼ **1c** < **1d** < **1e**) increases with increased planarization of the system, as is indicated by the θ values (Table 1). The red shifts of absorption maxima in compound series **2** and **3** also follow the order **e** > **c** > **f**. In all

(26) Yang, J.-S.; Chiou, S.-Y. Unpublished results.

(27) Gegiou, D.; Muszkat, K. A.; Fischer, E. *J. Am. Chem. Soc.* **1968**, *90*, 3907−3918.

(28) (a) Sander, R.; Stümpflen, V.; Wendorff, J. H.; Greiner, A. *Macromolecules* **1996**, *29*, 7705−7708. (b) Janić, I.; Kakaš, M. *J. Mol. Struct.* **1984**, *114*, 249−252.

(29) Subrayan, R. P.; Kampf, J. W.; Rasmussen, P. G. *J. Org. Chem.* **1994**, *59*, 4341−4345.

(30) Zerner, M. C.; Leow, G. H.; Kirchner, R. F.; Mueller-Westerhoff, U. T. *J. Am. Chem. Soc.* **1980**, *102*, 589−599.

Table 3. Results of the ZINDO Calculations for the Lowest Singlet States of **1a**−**f**

compd	excited state	Δ*E* (nm)	*f* [a]	description[b]
1a[c]	S_1	316	1.328	37:38 (0.95)
1b	S_1	319.4	1.335	43:44 (0.94)
1c	S_1	324.5 (324.4)[d]	1.443 (1.525)[d]	51:52 (0.89)
1d	S_1	329.5 (329.8)[d]	1.405 (1.478)[d]	54:55 (0.88)
1e	S_1	342.6	1.326	65:66 (0.85)
				65:69 (0.07)
	S_4	295.8	0.315	64:67 (0.10)
				65:67 (0.49)
				65:71 (0.17)
				65:72 (0.05)
1f	S_1	319.3 (319.0)[d]	1.435 (1.478)[d]	57:58 (0.93)

[a] Oscillator strength. [b] Orbital numbers of the pure configurations are given and the weight of each configuration is given in parentheses. Only configurations with 5% or greater contribution are included. [c] From ref 5. [d] Values in parentheses are for the anti conformer (eq 1).

cases, the absorption spectra undergo only small shifts with changing solvent polarity, indicating a small difference between the dipole moments of the ground and Franck−Condon (FC) excited states.

The electronic structure and spectra of **1a**−**f** have been further investigated by means of ZINDO calculations using the algorithm developed by Zerner and co-workers.[30] Ground-state molecular structures from the AM1 calculations were adopted. The calculated energies and oscillator strengths of the lowest excited singlet states (S_1) are reported in Table 3. Our calculations can reproduce the literature data for **1a**.[5] In the cases of **1c**, **1d**, and **1f**, data are reported for both syn and anti conformers. The results indicate that both conformers have virtually the same electronic character. The relative ZINDO-derived S_1 transition energies (**1a** < **1f** < **1b** < **1c** < **1d** < **1e**) and oscillator strengths (**1a** ∼ **1e** < **1b** < **1d** < **1f** < **1c**) agree well with the observed absorption spectra (Figure 1), although the calculated transition energies for **1b** are somewhat overestimated. Similar discrepancies between the observed and ZINDO calculated transition energies have been reported[11] for other *N*,*N*-dimethylaminoarenes.

The ZINDO-derived highest occupied molecular orbital (HOMO) and lowest unoccupied molecular orbital (LUMO) for **1a**, **1c**, and **1e** are shown in Figure 2. More detailed orbitals of **1a** have been documented,[5] and those of **1c** and **1e** are provided in the Supporting Information. In all three cases, the HOMO is localized primarily on the aminostyrene moiety, but there is a progressive change on going from **1a** to **1c** to **1e**, wherein the charge density is increased at the nitrogen atom but decreased at the central double bond.[31] On the other hand, the LUMO is localized on the stilbene moiety with nearly the same appearance in all three cases. These results suggest that the HOMO → LUMO transition has an increased amine → styrene charge-transfer character and a decreased antibonding character for the central double bond on going from **1a** to **1c** to **1e**. In addition, the introduction of *N*-phenyl substituents results in more extensive configuration interaction. Consequently, the contribution of the HOMO → LUMO configuration to the description of S_1 is reduced from >95% in **1a** to ∼85% in **1e** (Table 3). The other configurations that contribute to S_1 in **1c** and **1e** are transitions mainly localized in the diphenylamine or triphenylamine moiety. The higher energy absorption band of **1e** is calculated to be a consequence of $S_0 \rightarrow S_4$ with configurations all localized in the triphenylamine moiety (Table 3). The frontier orbitals of **1b** and **1f** resemble those of **1a**, and those of **1d** resemble those of **1c** (figures not shown). Unlike the cases of **1c**−**e**,[31] the *N*-phenyl group in **1f** plays nearly no role in the frontier orbitals. This can be attributed to the poor orbital overlap between the *N*-phenyl and the aminostilbene groups.

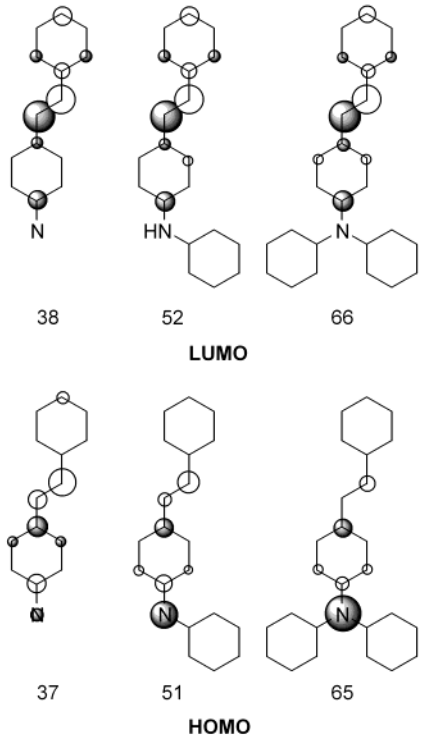

Figure 2. ZINDO-derived HOMO and LUMO for **1a**, **1c**, and **1e**. Only atomic charge densities with 5% or larger contribution are included.

Fluorescence Spectra. The fluorescence maxima (λ_{fl}), the half-bandwidth ($\Delta\nu_{1/2}$), the 0,0 transitions ($\lambda_{0,0}$), and the Stokes shift ($\Delta\nu_{st}$) of aminostilbenes **1**−**3** in hexane and acetonitrile are reported in Table 2. The 0,0 transitions were estimated from the intersection of normalized absorption and fluorescence spectra. No discernible change in the shape of the fluorescence spectra of **1c**−**f** was found when the excitation wavelength was varied from 290 to 370 nm.[21] In conjunction with the single-exponential fluorescence decay (vide infra), it is concluded that either one conformer predominates or both conformers have the same excited state behavior in the cases of structurally unsymmetrical aminostilbenes **1c**, **1d**, and **1f**. The same electronic structures are calculated by ZINDO for both syn and anti conformers of **1c**, **1d**, and **1f**, in accord with the latter situation. While the fluorescence spectra of **2** are essentially independent of the excitation wavelength, small differences in the fluorescence spectra can be observed in the cases of compound series **3**.[21] On the basis of the well-established rotational isomerism in the parent hydrocarbon of **3** (2-styrylnaphthalene),[32] this can be attributed to the different spectra of conformers that differ in naphthyl-vinyl conformation.

The fluorescence spectra of **1c**−**f** in hexane, which are shown in Figure 3 along with the spectra of **1a**[5] and **1b**,[16] display

(31) The contribution of charge density of the *N*-phenyl substituent(s) to the HOMO is ∼10% in **1c** and ∼25% in **1e**, but their contribution to the LUMO is negligible for both cases.

(32) Saltiel, J.; Sears, D. F., Jr.; Choi, J.-O.; Sun, Y.-P.; Eaker, D. W. *J. Phys. Chem.* **1994**, *98*, 35−46 and references therein.

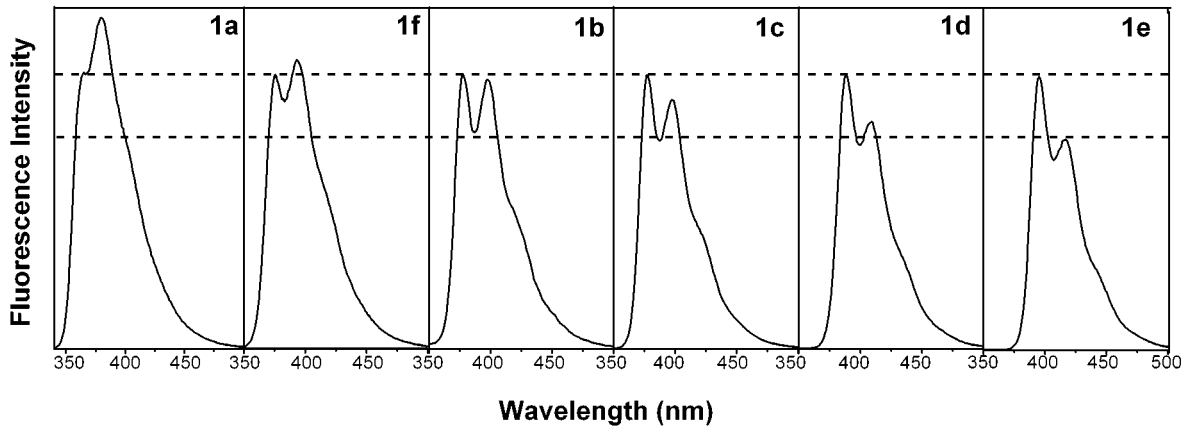

Figure 3. Fluorescence spectra of **1a**−**f** in hexane.

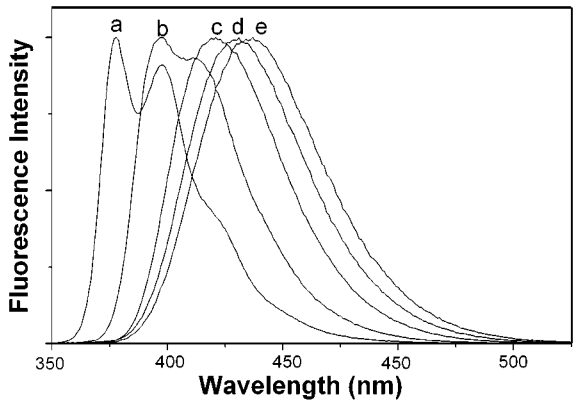

Figure 4. Fluorescence spectra of **1c** in (a) hexane, (b) toluene, (c) THF, (d) acetone, and (e) acetonitrile.

vibrational structure. The vibrational structure in all six aminostilbenes is 1300 ± 80 cm^{-1}, which is similar to that of *trans*-stilbene and can be attributed to the C=C stretching mode.[2] The spectra in Figure 3 are normalized according to the 0,0 band and arranged in an order of increased intensity ratio of 0,0 vs 0,1 band. According to the Franck−Condon principle, compounds with a less extent of structural distortion on going from the ground state to the excited state show a more intense 0,0 band.[33] Thus, the increased transition probability of the 0,0 bands in **1c**−**e** when compared with the other three species suggests that the structure of the fluorescent state, particularly in the region of the central double bond, is less distorted in **1c**−**e**. Along this line, the fluorescence half-bandwidth is narrower (Table 2). These spectral features are consistent with the results of ZINDO calculations, which suggest a reduced role for the central double bond in the lowest excited state of **1c**−**e**. This might be associated with their higher torsional barriers and lower quantum yields for trans → cis photoisomerization (vide infra). Similar variations in the 0,0 vs 0,1 bands are also found for compound series **2** and **3** in hexane.[21]

Figure 4 shows the normalized fluorescence spectra of **1c** in solvents of different polarity, which are typical for all aminostilbenes. Whereas vibrational structure can be observed in hexane, the spectra are broadened in toluene and are completely structureless in more polar solvents. Unlike the absorption spectra, the fluorescence maxima show a considerable red shift on going from hexane to acetonitrile, providing evidence for the charge-transfer character of the fluorescent singlet (CT*) state. The solvent-dependent shifts[34] can be used to determine the dipole moment of the excited state using the Lippert−Mataga equation (eq 2).[35]

Table 4. Ground and Excited-State Dipole Moments for **1a**−**f**

compd	solvatochromic slope (cm^{-1})[a]	μ_g (D)[b]	μ_e (D)[c]
1a	6641[d]	2.0	10.1
1b	11254[e]	2.0	12.9
1c	8987	1.3	14.6
1d	9960	1.6	15.4
1e	9502	0.5	14.5
1f	7573	1.6	13.6

[a] Calculated based on eq 2. [b] Calculated by ZINDO algorithm. [c] Values used for the radius of solvent cavity: 5 Å for **1a** and **1b** and 6 Å for **1c**−**1f**. [d] From ref 5. [e] From ref 16.

$$\Delta\nu_{st} = \nu_{abs} - \nu_{fl} = [2\mu_e(\mu_e - \mu_g)/hca^3]\Delta f$$

where

$$\Delta f = (\epsilon - 1)/(2\epsilon + 1) - (n^2 - 1)/(2n^2 + 1) \qquad (2)$$

where ν_{abs} and ν_{fl} are the absorption and fluorescence maxima, μ_g and μ_e are the ground and excited-state dipole moments, a is the solvent cavity radius in Å, ϵ is the solvent dielectric, and n is the solvent refractive index. The ground-state dipole moments (μ_g) are calculated using the ZINDO algorithm.[30] The values of the solvatochromic slopes for **1c**−**f** are reported in Table 4 along with the literature data for **1a** and **1b**. The excited-state dipole moments of **1a**−**f**, calculated from eq 2, are summarized in Table 4. Whereas the *N*-phenyl derivatives **1c**−**f** have smaller ground-state dipole moments when compared with **1a** and **1b**, their excited-state dipole moments are similar (**1f**) or even larger (**1c**−**e**). The former is expected based on the sum of component bond moments, and the latter is consistent with the prediction of ZINDO calculations that suggest a larger charge-transfer character for the *N*-phenyl derivatives in the lowest excited state (Figure 2).

(33) (a) Balzani, V.; Scandola, F. *Supramolecular Photochemistry*; Ellis Horwood: Chichester, 1991, Chapter 2. (b) Parker, C. A. *Photoluminescence of Solutions*; Elsevier: New York, 1968; pp 11−13.

(34) The Stokes shifts were determined in 10 solvents, including hexane, toluene, dichloromethane, diethyl ether, dibutyl ether, tetrahydrofuran, acetone, ethyl acetate, acetonitrile, and methanol,

(35) (a) Liptay, W. Z. *Z. Naturforsch.* **1965**, *20a*, 1441. (b) Lippert, E. *Z. Elecktrochem.* **1957**, *61*, 962−975. (c) Mataga, N.; Kaifu, Y.; Koizumi, M. *Bull. Chem. Chem. Soc. Jpn.* **1956**, *29*, 465−470.

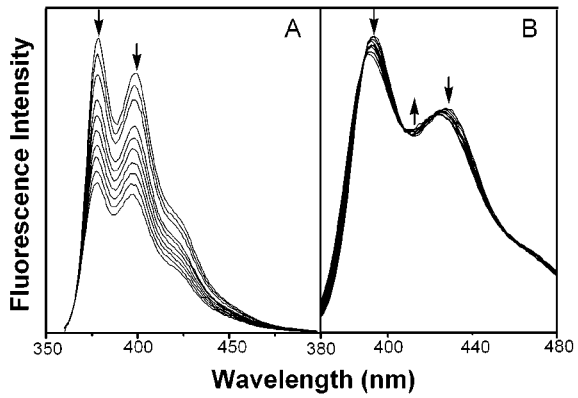

Figure 5. Temperature dependence of the fluorescence spectra of **1c** (A) and **1e** (B) in hexane recorded at an interval of 4 °C between 10 and 46 °C (top to bottom with increasing the temperature).

The temperature dependence of the fluorescence spectra of **1a**−**f** was studied in hexane between 10 and 46 °C. A significant reduction of the fluorescence intensity without changing the appearance of the spectra is observed for all aminostilbenes except **1e** upon heating from 10 to 46 °C (Figure 5A). This suggests that there are activated nonradiative decay processes that compete with fluorescence decay for **1a**−**d** and **1f**. In the case of **1e**, the fluorescence intensity is only slightly reduced and the spectra show a small blue shift ($\Delta\lambda_{0,0} = 2$ nm) upon heating from 10 to 46 °C (Figure 5B). The noticeable spectral shift for **1e** but not for the others with changing temperature indicates that the conformation of **1e** is more dependent upon the temperature, presumably due to the bulkier triphenylamine group that becomes less planar at higher temperature. Accordingly, the small fluorescence intensity variations for **1e** with changing temperature might be a consequence of temperature-induced conformational changes rather than the presence of weakly activated nonradiative decay processes.

Quantum Yields and Lifetimes. The fluorescence quantum yields (Φ_f) for aminostilbenes **1c**−**f** in hexane and acetonitrile were measured (Table 5). Values of Φ_f for **1c**−**e** in hexane are more than 1 order of magnitude larger than the values of $\Phi_f \sim 0.03$ reported[5,16] for **1a** and **1b**. The Φ_f values of **1c**−**e** decrease on going from hexane to acetonitrile, but the difference for **1e** is relatively small. On the other hand, fluorescence enhancement is either small (hexane) or negligible (acetonitrile) for **1f** vs **1a** or **1b**. Apparently, the geometry of the amino groups, defined by the θ and α values, is important in determining the fluorescence efficiency of the *N*-phenyl-substituted *trans*-4-aminostilbenes. The Φ_f value of compounds **2** and **3** is more sensitive to both amine substituents and solvent polarity than that of **1**. However, the relative fluorescence efficiencies among compound series **2** and **3** are parallel to those observed for **1** with the Φ_f values in the order of **e** > **c** > **f** > **a** (Table 5). Accordingly, the *N*-phenyl substituent effect on the fluorescence efficiency may be a general phenomenon for 4-amino-substituted stilbenes and 1,2-diarylethylenes.

Unconstrained *trans*-stilbene derivatives that have fluorescence as the dominant mode of excited-state decay ($\Phi_f > 0.5$) at room temperature has been limited to those with a few categories of substituent.[1−7,36] One category consists of 4,4′-disubstituted *trans*-stilbenes with strong electron-donating amino and methoxy groups.[7,17,36,37] The highly fluorescent 4,4′-diaminostilbene and its derivatives have long been employed as optical brighteners.[38] A second category is formed by *trans*-stilbenes with extended conjugation by aromatic π-substituents such as 4-phenylstilbene (4-styrylbiphenyl),[8] 4-styrylstilbene (1,4-bis(styryl)benzene),[9] 4,4′-diphenylstilbene,[39] and 2-stryl-naphthalene (**3**, A = H).[32] The third category was recently established for 3-amino-substituted *trans*-stilbenes and was attributed to "the *m*-amino effect".[4−6] The *N*-phenyl derivatives **1c**−**e** apparently represent a new category of strongly fluorescent *trans*-stilbenes. However, the "conjugated" nature of *N*-phenyl-amino and *N*,*N*-diphenylamino groups could be considered as "pseudo-π-substituents" belonging to the second category. In this context, it appears that resonance effects are more important than the electronic inductive effect of substituents in enhancing the fluorescence quantum yields of 4-monosubstituted *trans*-stilbenes.

Quantum yields for trans → cis photoisomerization (Φ_{tc}) of **1c**−**f** in hexane are reported in Table 5. Values of Φ_{tc} for **1c**−**e** are smaller than the values of $\Phi_{tc} \sim 0.5$ reported for *trans*-stilbene and **1a**.[5] The Φ_{tc} value of **1f** is larger than those of **1c**−**e** but smaller than that of **1a**, which is consistent with its intermediate Φ_f value in hexane. Assuming that the decay of the perpendicular p* state yields a 1:1 ratio of trans and cis isomers,[3] the sum of the fluorescence and isomerization quantum yields ($\Phi_f + 2\Phi_{tc}$) for **1c**, **1d**, and **1f** in hexane is within the

Table 5. Quantum Yields for Fluorescence (Φ_f) and Photoisomerization (Φ_{tc}), Fluorescence Decay Times (τ_f), Rate Constants for Fluorescence Decay (k_f) and Nonradiative Decay (k_{nr}), and Activation Energies (E_a) for Nonradiative Decay for **1**−**3**

compd	solvent	Φ_f	Φ_{tc}	τ_f (ns)	k_f (10^8 s^{-1})	k_{nr} (10^8 s^{-1})	E_a (kcal/mol)[f]
1a[a]	hexane	0.03[b]	0.49[c]	∼0.1[c]	3.0[b]	97[b]	3.6[b]
	acetonitrile	0.03	0.52	∼0.1	3.0	97	
1b[d]	hexane	0.03		∼0.1	3.0	97	3.6[b]
	acetonitrile	0.04		∼0.1	4.0	96	
1c	hexane	0.51	0.31[h]	0.34	15	14	4.9
	acetonitrile	0.30		0.39	7.7	18	
1d	hexane	0.64	0.18[h]	0.62	10	5.8	4.7
	acetonitrile	0.31		1.86	1.7	3.7	
1e	hexane	0.57	0.14[h]	0.51	11	8.4	0.87 (1.9)[g]
	acetonitrile	0.53		1.37	3.9	3.4	
1f	hexane	0.11	0.43	∼0.1	11	89	4.3
	acetonitrile	0.04		∼0.1	4.0	96	
2a[e]	cyclohexane	0.02		0.22	0.91	45	
	acetonitrile	0.03		0.18	1.7	54	
2c	hexane	0.37		0.29	13	22	
	acetonitrile	0.25		0.54	4.6	14	
2e	hexane	0.55		0.56	9.8	8.0	
	acetonitrile	0.39		1.52	2.6	4.0	
2f	hexane	0.08		∼0.1	8.0	92	
	acetonitrile	0.05		∼0.1	5.0	95	
3a[e]	cyclohexane	0.08		0.20	4.0	40	
	acetonitrile	0.05		0.23	2.2	41	
3c	hexane	0.46		0.34	14	16	
	acetonitrile	0.28		0.43	6.5	17	
3e	hexane	0.61		0.40	15	9.8	
	acetonitrile	0.42		1.09	3.9	5.3	
3f	hexane	0.20					
	acetonitrile	0.08		0.20	4	46	

[a] From ref 5, unless otherwise noted. [b] From this work. [c] In cyclohexane, from ref 5. [d] From ref 16, unless otherwise noted. [e] From ref 4. [f] Calculated based on eq 3 assuming $k_{isc}/k_f \sim 0$. [g] Based on I_f at 396 nm and the value in parentheses is obtained from $k_{isc}/k_f = 0.42$. [h] Containing 10% of THF by reason of solubility.

(36) Smit, K. J.; Ghiggino, K. P. *Chem. Phys. Lett.* **1985**, *122*, 369−374.
(37) Zeglinski, D. M.; Waldeck, D. H. *J. Phys. Chem.* **1988**, *92*, 692−701.
(38) Meier, H. *Angew. Chem., Int. Ed. Engl.* **1992**, *31*, 1399−1420 and references therein.
(39) Tan, X.; Gustafson, T. L. *J. Phys. Chem. A* **2000**, *104*, 4469−4474.

experimental error of 1.0, as is the case of **1a**, which suggests that other channels of nonradiative decay are negligible. Although the sum is somewhat lower than unity (0.85) for **1e**, other nonradiative decay pathways such as internal conversion[6] should be of relatively minor importance.

The fluorescence lifetimes (τ_f) of the aminostilbenes in both hexane and acetonitrile at room temperature are shown in Table 5. All decays can be well fit by single-exponential functions, although dual exponential fluorescence decay might be expected for **3** on the basis of the excitation wavelength-dependent fluorescence spectra.[21] A decay component comparable to or much shorter than those reported in Table 5 for **3** would not be resolved by our lifetime apparatus, which has a resolution of ~0.1 ns.[40] In accord with the larger fluorescence quantum yields, the lifetimes of **1c**−**e** are longer than those of **1a**, **1b**, and **1f**. However, unlike the Φ_f values, the τ_f values of **1c**−**e** are larger in acetonitrile vs hexane. Consequently, the fluorescence rate constants ($k_f = \Phi_f \tau^{-1}$) are smaller in acetonitrile (Table 5). The fluorescence rate constants of **1c**−**f**, when compared with those of **1a**, are larger in hexane but similar in acetonitrile. The overall nonradiative deactivation ($k_{nr} = 1/\tau_f - k_f$) was also calculated. Values of k_{nr} are lower for **1c**−**e** than **1a**, **1b**, and **1f**, which might account for the longer fluorescence lifetimes and the larger Φ_f values in the former cases.

Torsional Barriers. The temperature dependence of the fluorescence spectra (Figure 4) allows estimation of the activation energy (E_a) for nonradiative decay according to the equation[41,42]

$$\ln(I_f^o/I_f - 1 - k_{isc}/k_f) = \ln(A_0/k_f) - E_a/RT \qquad (3)$$

where I_f^o and I_f are the limiting fluorescence intensity and the fluorescence intensity measured at temperature T (K), k_{isc} is the rate constant for intersystem crossing, and A_0 is the Arrhenius constant. When intersystem crossing is negligible ($k_{isc}/k_f \sim 0$) in the excited singlet state decay, a linear Arrhenius plot of $\ln[(I_f^o/I_f) - 1]$ against $1/T$ will give an E_a value (slope $= -E_a/R$) for the nonradiative decay process. This plot requires several assumptions, including (1) constant solvent properties and k_f values for aminostilbenes **1a**−**f** over the temperature range of 10−46 °C, (2) a value of 1.0 for the limiting fluorescence quantum yield ($\Phi_f^o = 1.0$), and (3) $I_f^o = (\Phi_f^o/\Phi_f)I_f$ (295 K). The Arrhenius plots for **1a**−**f** are shown in Figure 6, and the corresponding E_a values are reported in Table 5. The E_a value of 3.6 kcal/mol provided by this method for **1a** in hexane is reasonably consistent with the value of $E_a \sim 3.5$ kcal/mol previously determined based on the temperature-dependent lifetime data.[5] In addition, the E_a value of 4.9 kcal/mol and k_{nr} value of $\sim 1.4 \times 10^9$ for **1c** in hexane corresponds to an Arrhenius constant (A_0) of $\sim 6 \times 10^{12}$, which agrees with the literature values of A_0 (10^{12}−10^{14}) for alkene isomerization.[3] The temperature-induced fluorescence shift in **1e** results in different intensity variations at different emission wavelengths (e.g., intensity decreased at 296 nm but increased at 308 nm) (Figure 5B). Thus, unlike those of **1a**−**d** and **1f**, the E_a values reported in Table 5 for **1e** should not be given much weight.

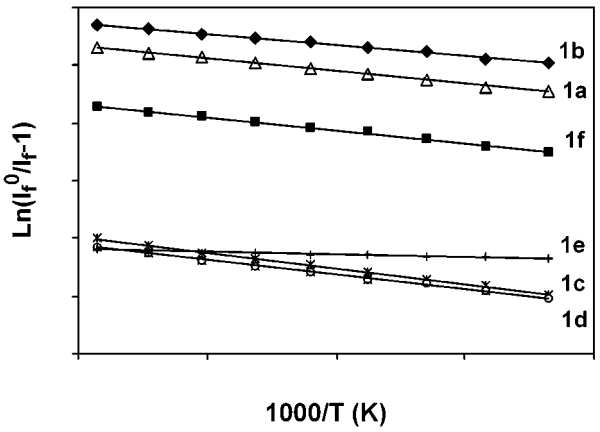

Figure 6. Arrhenius plots of the fluorescence efficiencies for **1a**−**f**.

Differences in the mechanism of photoisomerization of **1a**−**f** are indicated by their E_a values. The singlet-state mechanism of photoisomerization for *trans*-stilbene is attributed to both the small rate constant for intersystem crossing ($k_{isc} = 3.9 \times 10^7$ s^{-1}) and low barrier (~3.5 kcal/mol) for singlet-state ethylene torsional relaxation.[3] Aminostilbenes **1a** and **1b** have values of E_a, Φ_{tc}, Φ_f, and k_{nr} all similar to *trans*-stilbene and thus have been assumed to undergo photoisomerization mainly via the singlet excited state.[1−3,5,16] The singlet-state mechanism can also account for the smaller values of Φ_{tc} for **1c**, **1d**, and **1f** in hexane on the basis of the larger E_a values and the fact that intersystem crossing is normally an unactivated process for stilbenes.[1−3,41] Since intersystem crossing does not appear to compete with fluorescence and singlet torsion for aminostilbenes **1a**−**d** and **1f**, Φ_f should attain a value of 1.0 for them at low temperatures. This validates one of the assumptions required for estimating the E_a values by the plots shown in Figure 6. On the other hand, the value of E_a for **1e**, if present, is too small to account for the low Φ_{tc} and high Φ_f values by the singlet-state mechanism. It is thus concluded that **1e** undergoes photoisomerization via the triplet-state pathway, presumably due to the presence of a high excited singlet state torsional barrier. Assuming that the twisted triplet ($^3p^*$) decays to yield a 1:1 ratio of trans and cis isomers, quantum yields and rate constants for intersystem crossing can be estimated from the measured isomerization quantum yields and lifetimes ($\Phi_{isc} = 2\Phi_{tc}$, $k_{isc} = \Phi_{isc}\tau_f^{-1}$). The calculated value of k_{isc} for **1e** in hexane is 5.5×10^8 s^{-1}, which lies between the values for *trans*-stilbene (3.9×10^7 s^{-1}) and *trans*-4-bromostilbene (5.0×10^9 s^{-1}).[3] The larger value of k_{isc} for **1e** vs *trans*-stilbene might be a consequence of the reduced S−T energy gap, since the energy of the $^1t^*$ state of **1e** is ~14 kcal/mol lower than that of *trans*-stilbene based on their 0,0 transition energies (Table 2). Although an Arrhenius plot of $\ln[(I_f^o/I_f) - 1.42]$ against $1/T$ (eq 3) might be more appropriate for **1e** than the one shown in Figure 6 due to the conclusion of a triplet-state photoisomerization mechanism, this does not provide new information. As mentioned above, the observed small temperature dependence of fluorescence spectra for **1e** might be a consequence of weakly activated process of conformational changes, since the amine conformation defined by the parameters θ and α strongly affects the fluorescence quantum yields and excited singlet state energies of *N*-phenyl substituted stilbenes, as is demonstrated by the dramatic difference in Φ_f and λ_{fl} for **1c** vs **1f**. This argument is consistent with the fact of

(40) The results of biexponential fitting might not be reliable except for the case of **3e** in acetonitrile, which provides $\tau_1 = 0.55$ ns (11%) and $\tau_2 = 1.15$ (89%).
(41) Saltiel, J.; Marinari, A.; Chang, D. W.-L.; Mitchener, J. C.; Megarity, E. D. *J. Am. Chem. Soc.* **1979**, *101*, 2982−2996.
(42) Sakurovs, R.; Ghiggino, K. P. *Aust. J. Chem.* **1981**, *34*, 1367−1372.

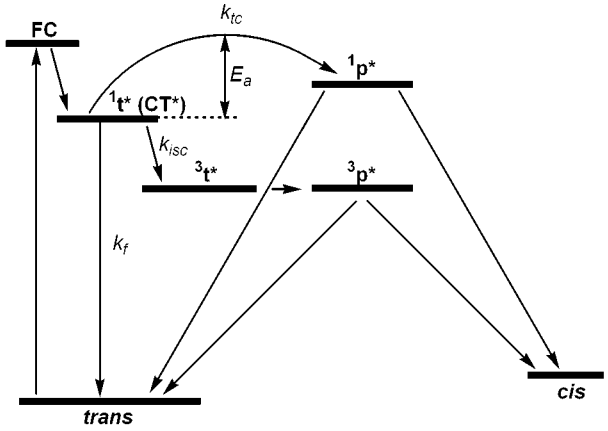

Figure 7. Simplified scheme for the formation and decay of the fluorescent CT* (^{1}t*) state of aminostilbenes **1a**−**f**.

$\Phi_f + 2\Phi_{tc} < 1$ for **1e**, which suggests the presence of a minor nonradiative decay pathway other than intersystem crossing. The photochemical behavior of aminostilbenes **1a**−**f** is summarized by a simplified scheme shown in Figure 7.

Apparently, the large increase in fluorescence quantum yields for **1c**,**d** vs **1a**,**b** results not only from the modest increase in the singlet torsional barrier (ΔE_a = 1.1−1.3 kcal/mol), but also from the increased radiative decay rate constants ($\Phi_f = k_f/(k_f + k_{nr})$). Likewise, the triplet-state photoisomerization for **1e** results not only from the large barrier for singlet torsion, but also from the increased rate constant for intersystem crossing, which is comparable with that for fluorescence (Table 5). A similar situation has recently been proposed for 4,4′-diaminostilbene and its tetramethyl derivative.[7] Photoisomerization via the triplet state as a consequence of a large barrier for singlet torsion was reported for 3-aminostilbene and its disubstituted derivatives;[5−7] however, the comparable values of k_f and k_{isc} in these cases result from decreased rate constants for fluorescence instead of increased rate constants for intersystem crossing. Such an origin of triplet-state photoisomerization for aminostilbenes is apparently different from that for some nitro-, bromo-, or carbonyl-substituted *trans*-stilbenes, which have large rate constants for intersystem crossing (k_{isc} ∼10^9−10^{10} s^{-1}) as a result of either the introduction of a low-lying n,π^* state or an internal heavy atom effect.[1−3]

The increase of barrier height for singlet torsion in **1c**−**e** suggests that the introduction of the *N*-phenyl group lowers the energy of the ^{1}t* state more than that of ^{1}p*.[5] The relative energies of ^{1}t* can be estimated from the position of their 0,0 transitions (Table 2). When compared with that of **1a**, the 0,0 energies of **1c**−**f** are lower by approximately 3, 5, 7, and 2 kcal/mol, respectively. Estimation of the energy of the ^{1}p* state is not so straightforward. The nature of the ^{1}p* state for single alkenes is not well defined but has been described as a resonance hybrid of biradical and charge-transfer configurations (eq 4).[43]

$$\psi_{p^*} = c_1\,\psi_{\text{biradical (A•B•)}} + c_2\,\psi_{\text{CT (A+B−)}} + c_3\,\psi_{\text{CT (A−B+)}} \quad (4)$$

An electron-donating or electron-withdrawing substituent at the 4-position of stilbene would be expected to stabilize one of the two charge-transfer configurations and thus lower the energy of ^{1}p*. For *trans*-stilbene, the ^{1}t* and ^{1}p* states have been shown to be approximately isoenergetic.[44] The similar quantum yields of fluorescence and photoisomerization for *trans*-stilbene, **1a**, and **1b**,[3,5,16] thus indicate that both amino and *N*,*N*-dimethylamino substituents stabilize the ^{1}t* and ^{1}p* states to a similar extent. Accordingly, the *N*-methyl (or more likely *N*-alkyl in general) groups stabilize the ^{1}p* state as well as the ^{1}t* state, whereas the *N*-phenyl groups stabilize the ^{1}t* state more than the ^{1}p* state.

The larger stabilization of *N*-phenyl substituents to the ^{1}t* vs ^{1}p* states of 4-aminostilbenes can be rationalized by a model based on Lewis resonance structures, which was originally proposed to rationalize the large singlet torsional barrier (>7 kcal/mol) for 3-amino-substituted *trans*-stilbenes.[5,6] As is depicted below for **1c**, the *N*-phenyl substituent provides an additional resonance structure for the planar ^{1}t* state (eq 5) but not for the twisted ^{1}p* state (eq 6).

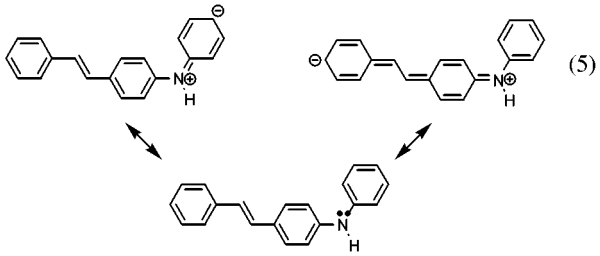

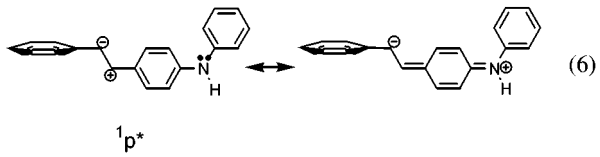

Likewise, there are two more resonance structures for the ^{1}t* but not the ^{1}p* state in the case of **1e**, which further lowers the energy of ^{1}t* and further raises the singlet torsional barrier. The lower ^{1}t* state of **1d** vs **1c** is a consequence of the introduction of the *N*-methyl group. Since an *N*-methyl group provides a similar extent of stabilization to both ^{1}t* and ^{1}p* states, it is as expected that the singlet torsional barrier for **1c** and **1d** should be similar (Table 5). The different effects of the *N*-phenyl vs the *N*-methyl substituent on the ^{1}p* state are further supported by comparison of **1b** and **1c**. The absorption maxima and 0,0 transition (^{1}t*) energies of **1b** and **1c** are essentially identical, but their singlet torsional barrier and fluorescence quantum yields in hexane are quite different (Table 5). Figure 8 depicts the potential energy for ethylene bond torsion in the lowest excited state for **1a**−**f** in hexane.

Concluding Remarks

The strongly fluorescent nature of the *N*-phenyl and *N*,*N*-diphenyl derivatives of *trans*-4-aminostilbene is borne out by our detailed studies on the excited-state behavior of aminostilbenes **1c**−**f**. The introduction of *N*-phenyl substituents extends the "conjugation" length of aminostilbenes and lowers the energy of the fluorescent ^{1}t* state, but it does not provide the same amount of resonance stabilization to the twisted ^{1}p* state. Consequently, the *N*-phenyl substituents stabilize the ^{1}t* state

(43) Bonačić-Koutecký, V.; Köhler, J.; Michl, J. *Chem. Phys. Lett.* **1984**, *104*, 440−443.

(44) Saltiel, J.; Waller, A. S.; Sears, D. F., Jr. *J. Am. Chem. Soc.* **1993**, *115*, 2453−2465.

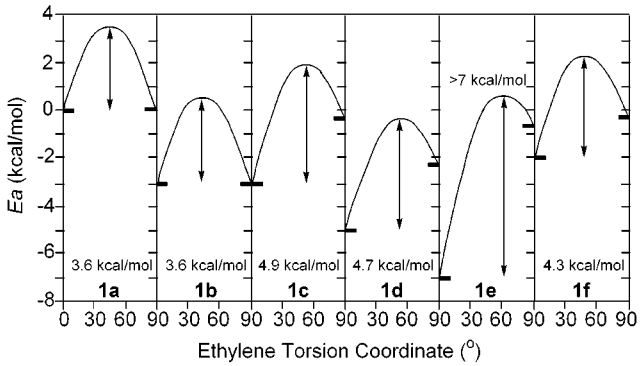

Figure 8. Potential energy diagram for ethylene bond torsion in the lowest excited state for **1a**−**f** in hexane. Energies are relative to ^{1}t* for **1a**.

more than the ^{1}p* state, leading to an increase of the singlet torsional barrier and thus a decrease of rate constants for photoisomerization. It is interesting to note that relatively small increases in the singlet torsional barrier (<1.5 kcal/mol) result in a large increase in Φ_f and decrease in Φ_{tc}. Since the amine nitrogen lone pair mediates the interactions between the *N*-phenyl and the stilbene groups, the geometry of the amine moiety determines the extent of "conjugation" interactions. For previously reported 4-monosubstituted *trans*-stilbenes, only π-conjugated substituents such as phenyl[8,39] and styryl[9] groups can significantly enhance the fluorescence quantum yields. Our results indicate that the *N*-phenylamino and *N*,*N*-diphenylamino groups behave as "nonconventional" π-conjugated substituents. Thus, we attribute the fluorescence enhancement in *trans*-4-aminostilbene upon *N*-phenyl substitutions to "the amino conjugation effect". Indeed, the concept of the amino conjugation effect has recently gained much attention in materials chemistry from the comparison of the properties of arylamines with *N*-phenyl vs *N*-alkyl substitutions.[10−14] Since fluorescence efficiency is an important issue for the development of organic light-emitting materials, the fluorescence enhancement of **1c**−**e** vs **1b** provides a new example showing the superior performance of *N*-phenyl vs *N*-alkyl substituents.

Insights into the amino conjugation effect on both photoisomerization and fluorescence have been gained from our systematic investigation of the amine substituents **a**−**f**. The ^{1}t* states of **1a**−**f** are all calculated to be of relatively pure HOMO → LUMO character. However, extending the conjugation of the whole molecular system with *N*-phenyl substituents imposes charge redistribution, leading to decreased charge densities at the central ethylene portion in the HOMO and thus reduced antibonding character for the central ethylene bond in the excited singlet state. One line of evidence is nicely provided by the progressive changes on the vibronic structures of fluorescence spectra of **1a**−**f** in hexane, which suggests a lesser extent of structural distortion for the strongly fluorescent *N*-phenyl derivatives **1c**−**e** in the excited state. Extending the conjugation to the *N*-phenyl substituents also increases the charge-transfer character in the ^{1}t* state on going from **1a** to **1c** to **1e**. Such differences in the ^{1}t* states of **1a**−**f** should be strongly associated with the efficiencies of both photoisomerization and fluorescence. It should be noted that the correlation between the relative fluorescence intensity ratio of the 0,0 to the 0,1 band and the excited-state structures of *trans*-stilbenes might be appropriate for a series of related substituents but not for those with different types or positions of substituents. In addition, the decreased decay process of singlet torsion might not be completely compensated by enhanced fluorescence, because other nonradiative decay pathways can compete with fluorescence. A switch of photoisomerization pathway from the singlet-state mechanism to the triplet-state one on going from **1c** and **1d** to **1e** clearly demonstrates this point. As a result of intersystem crossing, the second *N*-phenyl substituent in **1e** does not result in a larger fluorescence enhancement than the *N*-methyl group in **1d**.

Although less information is available for the stilbenoid systems **2** and **3**, the discussion for **1** might also apply to these two cases on the basis of their similar and parallel spectroscopic properties. We are currently investigating the *N*-phenyl substituent effect on the excited-state behavior of several other stilbenoid systems. Our preliminary results indicate that fluorescence enhancement by *N*-phenyl substitutions is a general phenomenon for *trans*-4-aminostilbenoid systems. Such a strongly fluorescent, conformation-dependent nature of *N*-phenyl substituent effect might be useful for the design of new stilbene-based fluorescent probes[45] and light-emitting materials.[19,28a,46]

Experimental Section

Methods. ^{1}H NMR and ^{13}C NMR spectra were recorded in $CDCl_3$ solution using a Bruker DRX-200 spectrometer with TMS as internal standard. Infrared spectra were recorded on a Bruker VECTOR 22 spectrometer. Elemental analyses and mass spectra were determined by the Instrumentation Center of National Cheng-Kung University or by that of National Taiwan University. UV spectra were measured on a Jasco V-530 double beam spectrophotometer. Fluorescence spectra were recorded on a PTI QuantaMaster C-60 spectrofluorometer at room temperature. A cell holder that allows for internal circulation was connected to a circulating bath with temperature variation of ±0.05 °C and used to obtain fluorescence spectra in the 10−46 °C temperature range. Anthracene (Φ_f = 0.27 in hexane)[47] was used as standard for the fluorescence quantum yield determinations (λ_{ex} = 338 nm) with solvent refractive index correction. The optical density of all solutions was about 0.1 at the wavelength of excitation. All fluorescence spectra are uncorrected and an error of ±10% is estimated for the fluorescence quantum yields. Fluorescence decays were measured at room temperature by means of an Edinburgh photon counting apparatus (OB900−14A) with a gated hydrogen arc lamp using a scatter solution to profile the instrument response function. The goodness of nonlinear least-squares fit was judged by the reduced χ^2 value (<1.3 in all cases), the randomness of the residuals, and the autocorrelation function. Quantum yields of photoisomerization were measured on optically dense degassed solutions (~10^{-3} M) at 313 nm using a 75 W Xe arc lamp and monochromator. *trans*-Stilbene was used as a reference standard (Φ_{tc} = 0.50 in hexane).[48] The extent of photoisomerization (<10%) was determined using HPLC analysis (HP1100, Whatman Partisil M9, 10/25, solvent gradient starting with hexane and ending at hexane:dichloromethane = 1:2). The reproducibility error was <15% of the average. MOPAC-AM1 and INDO/S-CIS−SCF (ZINDO) calculations were performed on a personal computer using the algorithms supplied by the package of Quantum CAChe Release 3.2,

(45) For examples of stilbene-based probes, see: (a) Lednev, I. K.; Hester, R. E.; Moore, J. N. *J. Am. Chem. Soc.* **1997**, *119*, 3456−3461. (b) Létard, J. F.; Lapouyade, R.; Rettig, W. *Pure Appl. Chem.* **1993**, *65*, 1705−1712. (c) Löhr, H.-G.; Vögtle, F. *Acc. Chem. Res.* **1985**, *18*, 65−72.
(46) Examples of stilbene-based light-emitting dendrimers: (a) Díez-Barra, E.; García-Martínez, J. C.; Riánsares del Rey, S. M.; Rodríguez-López, J.; Sánchez-Verdú, P.; Tejeda, J. *J. Org. Chem.* **2001**, *66*, 5664−5670. (b) Segura, J. L.; Gómez, R.; Martín, N.; Guldi, D. M. *Org. Lett.* **2001**, *3*, 2645−2648. (c) Pillow, J. N. G.; Halim, M.; Lupton, J. M.; Burn, P. L.; Samuel, I. D. W. *Macromolecules*, **1999**, *32*, 5985−5993.
(47) Birks, J. B. *Photophysics of Aromatic Molecules*; Wiley-Interscience: London, 1970.
(48) Malkin, S.; Fischer, E. *J. Phys. Chem.* **1964**, *68*, 1153−1163.

a product of Fujitsu Limited. The synthesis and characterization of compounds **1**−**3** are provided in Supporting Information.

Acknowledgment. Financial support for this research was provided by the National Science Council of Taiwan, ROC. We greatly appreciate Professor K. C. Hwang (NTHU) and Miss L. A. Dai for obtaining the lifetime data, Professor W.-R. Lee (NCU) for using his HPLC apparatus, Professor F. D. Lewis (Northwestern University) for helpful discussions, and the reviewers for helpful comments.

Supporting Information Available: Detailed synthetic procedures and product characterization data, ZINDO calculated frontier orbitals for **1c** and **1e**, Lippert−Mataga plots according to eq 2 for **1c**−**f**, fluorescence spectra of **1**−**3** in hexane recorded with different excitation wavelengths, and fluorescence spectra of compound series **2** and **3** in hexane (PDF). This material is available free of charge via the Internet at http://pubs.acs.org.

JA016416+